From $\mathbb{Z}_3$ Rabi model to Potts model

Anatoliy I. Lotkov,[1] Valerii K. Kozin,[1] Denis V. Kurlov,[1] Jelena Klinovaja,[1] and Daniel Loss[1]

[1] *Department of Physics, University of Basel, Klingelbergstrasse 81, CH-4056 Basel, Switzerland*

We study the $\mathbb{Z}_3$-symmetric Rabi models in this paper. In particular, we consider 1-mode and 2-mode variants of the $\mathbb{Z}_3$ Rabi model and determine their spectra. Next, we derive a mapping of the 2-mode $\mathbb{Z}_3$ Rabi model onto a qubit-boson ring. This mapping allows us to formulate a possible implementation of the $\mathbb{Z}_3$ Rabi model based on superconducting qubits and provides a context for the previously proposed optomechanical implementation. Furthermore, we propose a physical implementation of the $\mathbb{Z}_3$ Potts model via a chain of $\mathbb{Z}_3$ Rabi models coupled through nearest-neighbor interactions. Finally, we investigate the effects of the disorder on these systems.

I. INTRODUCTION

$\mathbb{Z}_n$-symmetric systems have attracted attention in integrable models, topological phases, and quantum information. in integrable systems research, the $\mathbb{Z}_n$ symmetric Potts model plays an important role, being the nontrivial generalization of the simplest integrable systems like the Ising model or the XXZ model [1–4]. $\mathbb{Z}_n$ symmetry also arises in topological phases: parafermionic edge modes—generalizations of Majorana modes—inherit it naturally [5–9]. Finally, $\mathbb{Z}_n$ symmetry is useful for applied quantum technology, where qudit-based processors extend the usual qubit paradigm [10–15]. Besides, modern platforms for quantum computations, such as trapped ions or superconducting qubits, inherently possess more than 2 energy levels that can be used for the computation. And systems based on n-level qudits unavoidably bear $\mathbb{Z}_n$ symmetry.

For the sake of simplicity, we focus on the $\mathbb{Z}_3$ case; all results generalize readily to $\mathbb{Z}_n$ case. The main topic of this paper is the $\mathbb{Z}_3$ Rabi model. The usual $\mathbb{Z}_2$ Rabi model being one of the simplest quantum models is ubiquitous in modern condensed matter physics [16–19]. Hence, it is therefore natural to study its $\mathbb{Z}_n$ generalization, which has recently drawn interest [20–22]. We also discuss several variants of the $\mathbb{Z}_3$ Rabi model, their similarities and differences.

In particular, the model exhibits behavior similar to the superradiant phase found in the ordinary Rabi model. While a formal proof remains open, we present evidence for the existence of this phase transition. In the relevant regime, the ground state becomes a n-fold generalization of the cat state. A renewed interest in cat state research has emerged due to its proposed application as a Quantum Error Correction Code [23–26]. Cat states based on a two-photon dissipation boson system were even proposed as a platform for fault-tolerant quantum computation [27]. However, cat-state quantum error correction has focused on qubits. In this work, by achieving 3-fold cat states, we extend it to qudits by realizing $\mathbb{Z}_3$ cat states.

We then present a method to experimentally implement the $\mathbb{Z}_3$ Rabi model in variouis physical platforms, illustrated by superconducting qubits. To our knowledge, it is the first proposal to realize the $\mathbb{Z}_3$ Rabi model experimentally. We exploit discrete rotational symmetry of 1-dimensional finite systems with periodic boundary conditions as a source of $\mathbb{Z}_n$ symmetry. We also discuss why more straightforward approaches to implement the $\mathbb{Z}_n$ Rabi model do not work.

Next, a generalization of Hwang's proposal to build an Ising model by coupling a chain of $\mathbb{Z}_2$ Rabi models [28] allows us to combine a chain of $\mathbb{Z}_3$ Rabi models into a $\mathbb{Z}_3$ Potts model. As far as we know, quantum Potts models are also yet to be implemented in the experiment, except by simulating on a universal quantum computer. However, recently another realization based on Josephson junctions was proposed [29]. Hence, we believe our proposal could be of interest.

Additionaly, the Potts model is dual to a parafermion chain [30]. In particular, the chiral Potts model, i.e., a chain of Rabi models coupled chirally, exhibits already mentioned parafermion edge modes [5, 6]. Although we only briefly touch on the parafermion edge modes in this paper, we believe that a further investigation in this direction could be fruitful.

In the remainder of the manuscript we proceed as follows. In Sec. II, we introduce the 1-mode $\mathbb{Z}_n$ and $\mathbb{Z}_3$ Rabi models and study their properties. Next, in Sec. III, this construction is generalized to the 2-mode $\mathbb{Z}_3$ Rabi model. In Sec. IV, the 2-mode $\mathbb{Z}_3$ Rabi model is mapped to a qubit-boson ring of length 3. It allows us to propose superconducting-circuit and optomechanical implementations of the model. In Sec. V, the nearest-neighbour $\mathbb{Z}_3$ Potts model is built from a chain of $\mathbb{Z}_3$ Rabi models. In Sec. VI we analyze the impact of the disorder on the proposed construction. We conclude in Sec. VII.

II. $\mathbb{Z}_3$ RABI MODEL.

A. Qubit–boson ring

In this section we demonstrate how the two–mode $\mathbb{Z}_3$ Rabi model emerges in the single–excitation sector of a three–site qubit–boson (QB) ring with nearest–neighbour coupling. Superconducting and optomechanical implementations are briefly commented on, while a compact derivation for a general interaction matrix is deferred to Sec. A. Throughout we follow the notation of the main

text and retain only the steps essential for the specific form of the interaction.

The QB ring Hamiltonian is

$$\begin{aligned}\hat{H}_{\rm QB} &= \epsilon\sum_{j=0}^{2}\sigma_j^z + \Omega_{\rm QB}\sum_{j=0}^{2}\hat{a}_j^\dagger\hat{a}_j + \hat{V}_{\rm QB},\\ \hat{V}_{\rm QB} &= g\sum_{j=0}^{2}\big(\sigma_j^+\sigma_{j+1}^- e^{i(\hat{x}_j-\hat{x}_{j+1})} + \text{h.c.}\big),\end{aligned} \tag{1}$$

where $\Omega_{\rm QB}$ is the boson frequency and $m_{\rm QB}$ the effective mass. Creation and annihilation operators are defined in the usual way,

$$\hat{a}_j = \sqrt{\frac{m_{\rm QB}\Omega_{\rm QB}}{2}}\,\hat{x}_j + i\sqrt{\frac{1}{2m_{\rm QB}\Omega_{\rm QB}}}\,\hat{p}_j. \tag{2}$$

This is a variant of the model studied in Ref. [22].

Because $[\hat{H}_{\rm QB},\hat{S}^z]=0$ with $\hat{S}^z=\sum_j\sigma_j^z$, the number of spin excitations is conserved. We therefore focus on the single–excitation subspace

$$\mathcal{H}_{\rm QB,1} = \text{Span}\big\{|\uparrow\downarrow\downarrow\rangle, |\downarrow\uparrow\downarrow\rangle, |\downarrow\downarrow\uparrow\rangle\big\}. \tag{3}$$

a. Spin–dependent momentum translation. Applying the unitary operator $S=\prod_j e^{i\sigma_j^z\hat{x}_j/2}$ removes the exponentials in $\hat{V}_{\rm QB}$ and yields

$$\begin{aligned}S^{-1}\hat{H}_{\rm QB}S = \epsilon\sum_j\sigma_j^z + \Omega_{\rm QB}\sum_j\hat{a}_j^\dagger\hat{a}_j + \frac{1}{2m_{\rm QB}}\sum_j\hat{p}_j\sigma_j^z\\ + \frac{3}{4m_{\rm QB}} + g\sum_j\big(\sigma_j^+\sigma_{j+1}^- + \sigma_j^-\sigma_{j+1}^+\big).\end{aligned} \tag{4}$$

The qubit interaction is now purely spin–spin, at the price of an additional spin–boson term proportional to $\hat{p}_j\sigma_j^z$.

b. Discrete Fourier transform. Introducing momentum–space operators $\hat{a}(k)$ and spin operators $S^\pm(k)$ via the unitary (type-I) discrete Fourier transform, $\hat{a}(k)=\frac{1}{\sqrt{3}}\sum_j e^{-2\pi ijk/3}\hat{a}_j$ (and analogously for the spins), we bring Eq. (4) to

$$\begin{aligned}\hat{H}_{\rm FT} = \epsilon\sum_{k=0}^{2}S^z(k) + \Omega_{\rm QB}\sum_{k=0}^{2}\hat{a}^\dagger(k)\hat{a}(k) + \frac{3}{4m_{\rm QB}}\\ + \frac{1}{2m_{\rm QB}}\sum_{k=0}^{2}\hat{p}(k)S^z(-k) + g\sum_{k=0}^{2}\big(S^+(k)S^-(-k) + \text{h.c.}\big),\end{aligned} \tag{5}$$

which is block-diagonal in the crystal momentum k.

c. Restriction to $\mathcal{H}_{QB,1}$. Inside the single–excitation subspace the zero-momentum ($k=0$) boson mode decouples from the dynamics. Discarding constants and the inert mode we obtain

$$\begin{aligned}\hat{H}_{\rm QB,1} = \Omega_{\rm QB}\sum_{k=1}^{2}\hat{a}^\dagger(k)\hat{a}(k) + g\big(X+X^\dagger\big)\\ + i\sqrt{\frac{\Omega_{\rm QB}}{6m_{\rm QB}}}\Big[-(\hat{a}(1)-\hat{a}^\dagger(2))Z - (\hat{a}(2)-\hat{a}^\dagger(1))Z^\dagger\Big].\end{aligned} \tag{6}$$

d. Final rearrangement. A Hadamard transform on the spin degrees of freedom, combined with a global bosonic $U(1)$ phase rotation, brings the Hamiltonian to the canonical $\mathbb{Z}_3$ two–mode Rabi form,

$$\begin{aligned}\hat{H}_{\rm R2} = \Omega_{\rm QB}\big(\hat{a}^\dagger(1)\hat{a}(1)+\hat{a}^\dagger(2)\hat{a}(2)\big) + g\big(Z+Z^\dagger\big)\\ - \sqrt{\frac{\Omega_{\rm QB}}{6m_{\rm QB}}}\Big[(\hat{a}(1)+\hat{a}^\dagger(2))X + (\hat{a}(2)+\hat{a}^\dagger(1))X^\dagger\Big].\end{aligned} \tag{7}$$

The identification with Eq. (**??**) is

$$\Omega_R = \Omega_{\rm QB},\quad B=g,\quad \phi=0,\quad \lambda=\sqrt{\frac{\Omega_{\rm QB}}{6m_{\rm QB}}}. \tag{8}$$

For completeness we record the explicit "magnetic" term,

$$g\big(Z+Z^\dagger\big) = \begin{pmatrix}2g & 0 & 0\\ 0 & -g & 0\\ 0 & 0 & -g\end{pmatrix}. \tag{9}$$

Thus the two–mode $\mathbb{Z}_3$ Rabi model faithfully captures the dynamics of the QB ring in the single–excitation sector.

We emphasise superconducting qubits as a natural platform for engineering the interaction (1), although analogous constructions are possible in, for example, optomechanical settings.

1. *Why so complicated?*

The implementation of the $\mathbb{Z}_3$ Rabi model proposed in the previous section is considerably more complicated than the usual $\mathbb{Z}_2$ Rabi model implementations. To obtain the $\mathbb{Z}_2$ Rabi model it is enough to simply couple a qubit with a boson in a naive way. Therefore, one may wonder if these complications are needed. However, the straightforward generalization of the $\mathbb{Z}_2$ Rabi model to higher Rabi models does not work due to fundamental obstacles. It turns out to be considerably more difficult to get a $\mathbb{Z}_3$ symmetric interaction. In this section, we try to explain why.

There are two most common ways to get a two-level quantum system. It is possible to use a spin as a 2-level system [35–37] or two levels in anharmonic oscillator, e.g., the Rabi model describes a superconducting qubit coupled to a cavity in the ultra-strong coupling regime [38–44]. Therefore, it is simple to get a $\mathbb{Z}_2$ Rabi

model. It is enough to take either a spin or an anharmonic oscillator and couple it to a boson mode using $\hat{V} = \sigma_x \hat{x}_{\text{boson}}$.

Both ways are easily generalized to the $\mathbb{Z}_3$ Rabi model. To get a spin-based 3-level system we just need to take spin 1. However, in this case, we obtain an interaction through the spin-1 representation of s^x instead of X.

$$s^x = \begin{pmatrix} 0 & \sqrt{2} & 0 \\ \sqrt{2} & 0 & \sqrt{2} \\ 0 & \sqrt{2} & 0 \end{pmatrix} \tag{10}$$

It is easy to see that it is not $\mathbb{Z}_3$-symmetric. Hence, the spin 1/2 representation of the $SU(2)$ group is a convenient special case that, unfortunately, does not generalize. It does not mean that it is impossible to build a $\mathbb{Z}_3$ symmetric system out of spins as we have shown, or higher $\mathbb{Z}_n$ symmetric systems [45] in general. But it still explains why we need rather complicated ways to achieve it.

The second way to get a $\mathbb{Z}_2$ Rabi model is to use 2 levels of an anharmonic oscillator. Consequently, in the $\mathbb{Z}_2$ case σ^x operator is basically a restriction of the coordinate operator of the anharmonic oscillator $\hat{x}_{\text{an}} = (\hat{a}_{\text{an}} + \hat{a}^\dagger_{\text{an}})/\sqrt{2}$ to the two lowest levels. On the contrast, if we restrict it to 3-level system, we get

$$\hat{x}_{\text{an}} = \frac{1}{\sqrt{2}} \begin{pmatrix} 0 & \sqrt{1} & 0 \\ \sqrt{1} & 0 & \sqrt{2} \\ 0 & \sqrt{2} & 0 \end{pmatrix} \tag{11}$$

As a result, the $\mathbb{Z}_2$ Rabi model based on the anharmonic oscillator does not generalize to the higher $\mathbb{Z}_n$ Rabi models.

These obstacles make an experimental $\mathbb{Z}_n$-Rabi realization non-trivial, motivating our proposal.

The rationale provided in this section is in no way a formal proof. However, the argument should serve as an intuition as to why $\mathbb{Z}_3$ Rabi is less straightforward to engineer than its more well-known analogue. The model we proposed in the previous section solves this problem by having an inherent $\mathbb{Z}_3$ symmetry. It originates from the translational symmetry of a ring.

B. Superconducting circuit implementation

The obvious choice for boson modes is an LC circuit. For the qubit (σ_i) we consider superconducting charge qubits [46–49], because we want the qubit eigenstate to be a charge state. More extensive discussion on the charge qubits we use is provided in App. B. Here, we only want to comment that the qubit eigenstates are $|0\rangle, |1\rangle$ defined by $\hat{n}|0\rangle = 0$, $\hat{n}|1\rangle = |1\rangle$, where $\hat{n}$ is the capacitor charge operator. Below, to denote a linear span of these states we use $\mathcal{V}_k = \text{Span}\{|0\rangle_k, |1\rangle_k\}$ where k is the number of the qubit.

Fig. 1 shows a superconducting realization of the three-site qubit–boson ring. Each horizontal branch of

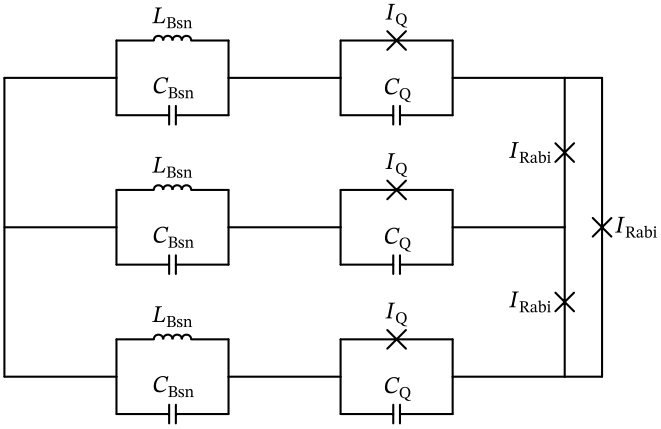

FIG. 1. Superconducting circuit implementation of the 2-mode $\mathbb{Z}_3$ Rabi model $\hat{H}_{\text{R2}}$. The LC circuits $(L_{\text{B}}, C_{\text{B}})$ host the boson modes; the charge qubits $(I_{\text{Q}}, C_{\text{Q}})$ correspond to the qubit degrees of freedom; Josephson junctions I_{Rabi} are responsible for the interaction term in the qubit-boson ring. Altogether, the circuit is described by the Hamiltonian (1).

the circuit (Fig. 1) correspond to site $i = 0, 1, 2$ of the qubit-boson ring. The ith boson and qubit are implemented by the LC circuit and SC qubit on the ith branch respectively. The JJs on the on the vertical segments of the circuit on the right of Fig. 1 are responsible for the interaction term in H_{QB} (1) [50–54]. On Fig. 1 is, the characteristic parameters of every circuit element are also shown: LC circuit's conductor and inductor have capacitance C_{B} and inductance L_{B} respectively. The qubit's JJ and capacitance have critical current I_{Q} and capacitance C_{Q} respectively. The coupling JJs on the right have critical current I_{R}. For clarity, we omit any elements that are necessary for an actual experimental implementation, e.g., read-out resonators, flux-bias lines, and filtering components.

Next, we describe why this circuit models the Hamiltonian (1). Without the coupling JJs, the LC circuits and qubits are independent from each other and are described by a non-interacting Hamiltonian:

$$\hat{H} = \sum_{i=0}^{2} \hat{H}_{LC,i}(\phi_i, q_i) + \sum_{i=0}^{2} \hat{H}_{Q,i}(\varphi_i, n_i), \tag{12}$$

where ϕ_i, q_i are the magnetic flux and the capacitor charge of the ith LC circuit, while φ_i, n_i are the JJsuperconducting phase and capacitor charge of the qubit. The LC circuit Hamiltonian is obviously $H_{LC,i} = q_i^2/(2C) + \phi_i^2/(2L)$. Meanwhile, we leave the qubit Hamiltonian $\hat{H}_{Q,i}$ generic to allow different qubit types. However, we require the qubit to be a charge qubit and satisfy the following properties:

$$\hat{H}_Q\Big|_{\mathcal{V}} = \begin{pmatrix} \langle 0_i| \hat{H}_Q |0_i\rangle & \langle 0_i| \hat{H}_Q |1_i\rangle \\ \langle 1_i| \hat{H}_Q |0_i\rangle & \langle 1_i| \hat{H}_Q |1_i\rangle \end{pmatrix} = \epsilon \sigma_z, \tag{13}$$

where the qubit states $|0_i\rangle, |1_i\rangle$ are the charge operator eigenstates $\hat{q}_i |0_i\rangle = Q |1_i\rangle$, $\hat{q}_i |1\rangle_i = (Q+1) |1\rangle_i$ with

$Q \in \mathbb{Z}$. $\mathcal{V}_i = \mathrm{Span}\{|0_i\rangle, |1_i\rangle\}$ is a qubit Hilbert space, i.e, a computational subspace of the full Hilbert space of the qubit system $\hat{H}_{Q,i}$. Due to this property, the operator $e^{i\varphi_i}$ acts on the qubit subspace $\mathcal{V}_i$ as a raising operator:

$$e^{i\hat{\varphi}_i}\Big|_{\mathcal{V}_i} = \begin{pmatrix} \langle 0_i| e^{i\hat{\varphi}_i} |0_i\rangle & \langle 0_i| e^{i\hat{\varphi}_i} |1_i\rangle \\ \langle 1_i| e^{i\hat{\varphi}_i} |0_i\rangle & \langle 1_i| e^{i\hat{\varphi}_i} |1_i\rangle \end{pmatrix} = \sigma^+, \tag{14}$$

because $[e^{i\phi}, n] = e^{i\phi}$.

If we now connect the ith and $(i+1)$th circuit branches with a JJ, it creates a cycle in the circuit. As a result, the fluxes and the superconducting phases have to satisfy a requirement:

$$\hat{\phi}_i + \hat{\varphi}_i + \hat{\varphi}_R - \hat{\varphi}_{i+1} - \hat{\phi}_{i+1} = 2\pi N, \text{ where } N \in \mathbb{Z}. \tag{15}$$

In other words, the superconducting phase ϕ_R of the coupling JJ is not an independent degree of freedom. Therefore, for the corresponding term in the Hamiltonian we obtain:

$$\hat{V}_{\text{SC QB},j} = I_{\text{R}} \cos\left(\hat{\phi}_R\right) = I_{\text{R}} \cos\left(\hat{\phi}_j + \hat{\varphi}_j - \hat{\phi}_{j+1} - \hat{\varphi}_{j+1}\right). \tag{16}$$

As we are only interested in qubit states $|0\rangle_k$, $|1\rangle_k$, we restrict the JJ term $\hat{V}_{\text{SC QB},j}$ to the qubit Hilbert subspace $\mathcal{V}_j \otimes \mathcal{V}_{j+1}$:

$$\begin{aligned} &\hat{V}_{\text{SC QB},j}\Big|_{\mathcal{V}_j\otimes\mathcal{V}_{j+1}} = \\ &= \frac{I_{\text{Rabi}}}{2}\left(e^{i(\hat{\varphi}_j - \hat{\varphi}_{j+1})} e^{i(\hat{\phi}_j - \hat{\phi}_{j+1})} + h.c.\right)\Big|_{\mathcal{V}_j\otimes\mathcal{V}_{j+1}} \\ &= \frac{I_{\text{Rabi}}}{2}\left(e^{i(\hat{\varphi}_j - \hat{\varphi}_{j+1})}\sigma_j^-\sigma_{j+1}^+ + h.c.\right). \end{aligned} \tag{17}$$

Here we used the fact that $e^{\pm i\hat{\phi}}$ acts as a raising/lowering operator for the charge qubit: $e^{i\hat{\phi}}|_{\mathcal{V}} = \sigma^+$. Hence the need for charge qubits rather than flux or phase qubits.

The Josephson junction coupling between two pairs of an LC circuits and a charge qubits gives us precisely the interaction term we wanted. As a result, we conclude that the system depicted in Fig. 1 is described by the Hamiltonian (1). The qubit-boson ring couplings can be expressed by the circuit parameters:

$$\begin{aligned} &\epsilon = \frac{\delta}{2C_Q},\ \Omega_{QB} = \left(\sqrt{L_{\text{B}}C_{\text{B}}}\right)^{-1/2}, \\ &m_{QB} = C_{\text{B}},\ g = \frac{I_{\text{Rabi}}}{2}. \end{aligned} \tag{18}$$

For details of the ϵ computation, see App. B. Finally, applying Sec. *II A* argument we deduce that the circuit is described by the $\mathbb{Z}_3$ Rabi model.

C. Optomechanical implementation

Another possible physical platform for the $\mathbb{Z}_3$ Rabi model is an optomechanical system consisting of 3 spins whose vibrational modes are boson degrees of freedom. They are connected by a circular waveguide that acts as an interaction medium between the spins and the vibrational phonons (first proposed in [22]).

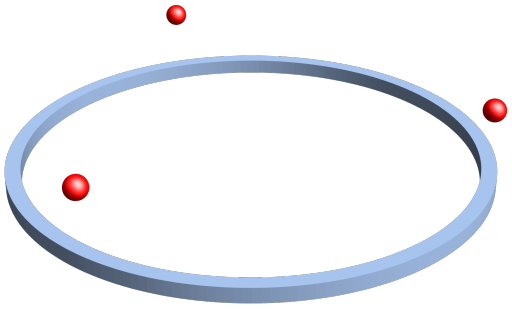

FIG. 2. Schematic illustration of the optomechanical implementation of the 2-mode $\mathbb{Z}_3$ Rabi model $\hat{H}_{\text{R2}}$ [22] The red spheres are trapped ions carrying two-level systems; their vibrational modes are the bosons from the qubit-boson ring. The blue ring is the chiral waveguide that facilitates the interaction in the qubit-boson ring. The system is described by the Hamiltonian $\hat{H}_{\text{OM}}$ (19).

Although challenging to realize, this platform illustrates the generality of our approach. In this section, we outline how the $\mathbb{Z}_3$ Rabi model arises in this model, for the extended discussion we refer the reader to the original paper [22].

The optomechanical model in question is described by the following Hamiltonian:

$$\begin{aligned} &\hat{H}_{\text{OM}} = \sum_{j=0}^{2}\zeta_j\hat{c}_j^\dagger\hat{c}_j + \epsilon\sum_{j=0}^{2}\sigma_j^z + \Omega_{\text{OM}}\sum_{j=0}^{2}\hat{a}_j^\dagger\hat{a}_j + \hat{V}_{\text{int}}, \\ &\hat{V}_{\text{int}} = \gamma\sum_{k,j=0}^{2}\left[\sigma_j^+\hat{c}_k e^{ik[R\phi_j + \hat{x}_j]} + \text{h.c.}\right], \end{aligned} \tag{19}$$

where $\zeta_k = vk$.

Using the Schrieffer-Wolff transformation [55], we can integrate out the photons degrees of freedom to get the Hamiltonian in the form we want:

$$\begin{aligned} &\hat{H}_{\text{OM,eff}} = \epsilon\sum_j\sigma_j^z + \Omega_{\text{OM}}\sum_j\hat{a}_j^\dagger\hat{a}_j \\ &-\frac{\gamma^2}{2v}\sum_{i<j}\left[i\sigma_i^+\sigma_j^- e^{iqR\phi_{ij}} e^{i\eta\left(\hat{a}_i + \hat{a}_i^\dagger - \hat{a}_j - \hat{a}_j^\dagger\right)} + \text{h.c.}\right]. \end{aligned} \tag{20}$$

The Hamiltonian is a bit different from (1). It is treated in App. **??** and gives rise to the following $\mathbb{Z}_3$ Rabi model:

$$\begin{aligned} &\hat{H}_{2\,\text{Rabi,mod}} = -\frac{\gamma^2}{2v}(e^{-5\pi i/6}Z + e^{5\pi i/6}Z^\dagger) \\ &+\Omega_{\text{OM}}(\hat{a}_1^\dagger\hat{a}_1 + \hat{a}_2^\dagger\hat{a}_2) \\ &-\frac{\Omega_{\text{OM}}^{1/2}\eta}{6^{1/2}}\left[(\hat{a}_1 + \hat{a}_2^\dagger)X + (\hat{a}_2 + \hat{a}_1^\dagger)X^\dagger\right] \end{aligned} \tag{21}$$

which differs from the $\mathbb{Z}_3$ Rabi model we acquired in the superconducting circuit context only by the $\mathbb{Z}_3$ "magnetic" term's phase $\varphi = -5\pi/6$.

We can explicitly write down the "magnetic" term

$$-\frac{\gamma^2}{2v}(e^{-5\pi i/6}Z + e^{5\pi i/6}Z^2) = \begin{pmatrix} \frac{\sqrt{3}\gamma^2}{2v} & 0 & 0 \\ 0 & -\frac{\sqrt{3}\gamma^2}{2v} & 0 \\ 0 & 0 & 0 \end{pmatrix}. \quad (22)$$

As one can see, the non-zero "magnetic" term's phase φ leads to all the eigenvalues being non-degenerate. Compare it to Eq. (9).

III. $\mathbb{Z}_3$ POTTS MODEL

A. Theoretical description

The $\mathbb{Z}_3$ Potts model [1] is a 1-dimensional chain of 3-level systems with a global $\mathbb{Z}_3$ symmetry. It originates from statistical physics as a straightforward generalization of the Ising model to more states on each site [1, 56]. Nowadays, the Potts model often appears in the context of qudit quantum computations [57, 58]. However, the direct experimental realization of the Potts model still does not exist. One of the goals of this paper is to propose such an experimental realization based on $\mathbb{Z}_3$ Rabi models. To achieve this, we generalize the idea of building an Ising model by coupling a chain of $\mathbb{Z}_2$ Rabi models, proposed by Hwang [28], to the $\mathbb{Z}_3$-symmetric case.

The $\mathbb{Z}_3$ Potts model Hamiltonian is

$$\begin{aligned}\hat{H}_{\text{Potts}} =& f_{\text{Potts}} \sum_{n=1}^{L} \left(e^{i\phi}Z_n + e^{-i\phi}Z_n^\dagger\right) \\ &+ J_{\text{Potts}} \sum_{n=1}^{L} \left(X_n X_{n+1}^\dagger + X_n^\dagger X_{n+1}\right).\end{aligned} \quad (23)$$

The first term just describes single-excitation energies, the second term is the $\mathbb{Z}_3$-symmetric nearest-neighbour interaction.

As we already discussed before, it is difficult to obtain a $\mathbb{Z}_3$ symmetry in an arbitrary 3-level system chain. But we have already learnt how to build a $\mathbb{Z}_3$ Rabi model. We use it as a building block for the $\mathbb{Z}_3$ Potts model, i.e., we want the 3 cat-states in the $\mathbb{Z}_3$ Rabi models (**??**) to serve as 3 states on the nth site of the Potts model $|j\rangle_n = |\psi_j\rangle_n$ for $j = 0, 1, 2$. By raising boson energy Ω_R in the Rabi model Hamiltonian (**??**) the higher energy states are effective decoupled from $|\psi_j\rangle$ states.

The main reason why it is convenient to build the Potts model from Rabi models is that the boson degrees of freedom in the Rabi models allow us to obtain a $\mathbb{Z}_3$ symmetric interaction. The reasoning is simple; the Rabi model's $\mathbb{Z}_3$ symmetry acting on bosons is a residue of a usual $U(1)$ boson symmetry. Consequently, if we take a $U(1)$ symmetric interaction of boson modes on neighbor sites, then it is by default be $\mathbb{Z}_3$ symmetric. And the simplest $U(1)$ symmetric boson interaction is just a hopping term $\hat{a}_n^\dagger \hat{a}_{n+1} + \text{h.c.}$ As a result, to obtain a $\mathbb{Z}_3$ Potts model we need to take a chain of $\mathbb{Z}_3$ Rabi models and couple them by the boson hopping term:

$$\begin{aligned}&\hat{H}_{\text{Rabi chain}} = \\ &\sum_{n=1}^{L} \hat{H}_{\text{Rabi},n} + J \sum_{n=1}^{L} \sum_{k=1}^{2} \left(\hat{a}_{n,k}^\dagger \hat{a}_{n+1,k} + \hat{a}_{n+1,k}^\dagger \hat{a}_{n,k}\right),\end{aligned} \quad (24)$$

where n is a chain-site subscript and k is a number of a boson mode in a $\mathbb{Z}_3$ Rabi model. We claim that this Hamiltonian gives us precisely the $\mathbb{Z}_3$ Potts model, when we restrict it to the Hilbert space $\bigotimes_n \mathcal{R}_n$ generated by the 3 cat states on the sites $n = 1, \ldots, L$.

Within the Rabi qutrit subspace, $\hat{a}_{n,k}$ acts as a permutation between the cat states:

$$\hat{a}_{n,k}|\psi_i\rangle_n = (\lambda/\Omega)|\psi_{i+1}\rangle_n. \quad (25)$$

For the creation operator it is a little bit more complicated:

$$\begin{aligned}&\hat{a}_{n,k}^\dagger|\psi_i\rangle_n = (\lambda/\Omega)|\psi_{i-1}\rangle_n + \delta, \text{ where} \\ &|\delta|^2 = 1.\end{aligned} \quad (26)$$

In the deep-strong coupling [59, 60] regime $\lambda/\Omega \gg 1$, we can neglect δ. As a result, in the Rabi qutrit subspace the creation/annihilation operators act as cyclic permutations: $\hat{a}_{n,k}|_{\mathcal{R}} = (\lambda/\Omega)X$, $\hat{a}_{n,k}^\dagger|_{\mathcal{R}} = (\lambda/\Omega)X^\dagger$. Consequently, in this sector the coupled Rabi chain is equivalent to the Potts model:

$$\begin{aligned}&J \sum_{k=0}^{2} \left(\hat{a}_{n,k}^\dagger \hat{a}_{n+1,k} + \hat{a}_{n+1,k}^\dagger \hat{a}_{n,k}\right) = \\ &3(\lambda/\Omega)^2 J \left(X_n^\dagger X_{n+1} + X_{n+1}^\dagger X_n\right).\end{aligned} \quad (27)$$

Therefore, we have $J_{\text{Potts}} = 3(\lambda/\Omega)^2 J$.

1. *Underlying qubit-boson ring*

Considering that the Rabi models in the chain are made from a qubit-boson ring, we need to show how to obtain the boson hopping interaction (**??**) in terms of the QB ring degrees of freedom.

It turns out to be quite simple. If we add hopping terms for the bosons in the qubit-boson chain, then it gives us the hopping term between the Rabi model bosons, because the Fourier transform does not change the form of the boson hopping interaction:

$$\begin{aligned}&\sum_{j=0}^{2} \left(\hat{a}_{n,j}^\dagger \hat{a}_{n+1,j} + \hat{a}_{n+1,j}^\dagger \hat{a}_{n,j}\right) \\ &= \sum_{k=0}^{2} \left(\hat{a}_{n,k}^\dagger \hat{a}_{n+1,k} + \hat{a}_{n+1,k}^\dagger \hat{a}_{n,k}\right)\end{aligned} \quad (28)$$

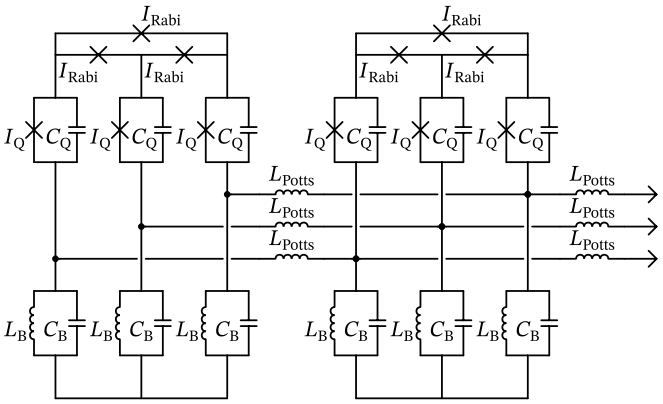

FIG. 3. Superconducting circuit implementation of the Potts model. The circuit is described by the Hamiltonian (24). Subscript "B" denote elements corresponding to boson degrees of freedom; subscript "Q" denote qubit elements; subscript "Rabi" denote elements responsible for interaction in qubit-boson ring; subscript "Potts" denote elements responsible for interaction in Potts model.

To simplify the notation, we do not use brackets here to denote the Fourier components of the boson modes. The subscript j correspond to the real space boson mode; the subscript k corresponds to the Fourier boson mode, i.e., the $\mathbb{Z}_3$ Rabi model boson modes. We have an extra term $\hat{a}_{n,0}, \hat{a}^\dagger_{n,0}$ which decouples the same way it did in Sec. II A.

The mapping between the parameters is the following:

$$f_{\text{Potts}} = g \exp\left(-\frac{1}{2m_{QB}\Omega_{QB}}\right), \qquad J_{\text{Potts}} = \frac{J}{2m_{QB}\Omega_{QB}}. \tag{29}$$

B. Coupled superconducting $\mathbb{Z}_3$ Rabi models

It is straightforward to implement the Potts model based on superconducting circuits. We consider a chain of superconducting circuits depicted in Fig. 1. Next, we need to couple the neighbor Rabi models with a boson hopping term to get the Hamiltonian (24). To do it, we couple the neighbor Rabi models using inductors (Fig. 3). Although capacitive coupling is more common, here it induces unwanted all-to-all coupling.

On the other hand, the inductor coupling leads us to the hopping term we want. First of all, the Hamiltonian terms corresponding to the inductors are:

$$\hat{V}_{\text{Potts},n} = \frac{1}{2L_{\text{Potts}}}(\hat{\phi}_{n+1} - \hat{\phi}_n)^2 = \frac{\hat{\phi}_n^2 + \hat{\phi}_{n+1}^2}{2L_{\text{Potts}}} + \frac{\hat{a}_n^\dagger \hat{a}_{n+1}^\dagger + \hat{a}_n^\dagger \hat{a}_{n+1} + \hat{a}_n \hat{a}_{n+1}^\dagger + \hat{a}_n \hat{a}_{n+1}}{L_{\text{Potts}} C_{\text{B}} \Omega_{QB}} \tag{30}$$

where we expressed the flux operator through the creation/annihilation operators $\hat{\phi}_n = (\hat{a}_n + \hat{a}_n^\dagger)/\sqrt{2C_{\text{B}}\Omega_{QB}}$.

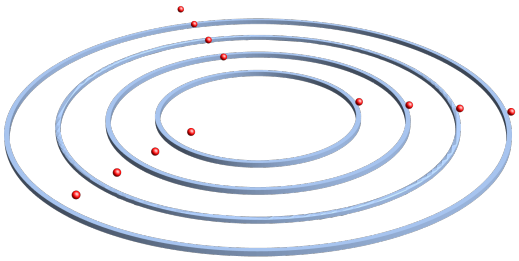

FIG. 4. Schematic illustration of the optomechanical (OM) implementation of the Potts model. It consists of several concentric OM implementations of the Rabi model, i.e., several concentric cyclic chiral waveguide and three trapped ions on top of each waveguide.

We ignore the $\hat{\phi}_n^2$ and $\hat{\phi}_{n+1}^2$ terms because they simply renormalize the Rabi model parameters. Additionally, the inductor coupling produces undesired terms $\hat{a}_n^\dagger \hat{a}_{n+1}^\dagger$ and $\hat{a}_n \hat{a}_{n+1}$. However, we can use Rotating Wave Approximation (RWA) to eliminate them. For the RWA to be applicable, we need $\Omega_{QB} = \sqrt{L_{\text{B}} C_{\text{B}}} \gg (L_{\text{Potts}} C_{\text{B}} \Omega_{QB})^{-1}$. After RWA we are left with the hopping term between the boson modes of the neighbor Rabi model. Consequently, in line with Sec. III A the superconducting circuit in question is modeled by the Potts model. The coupling parameters of the resulting Pottsd model could be expressed through the circuit parameters:

$$f_{\text{Potts}} = \frac{I_{\text{Rabi}}}{2} \exp\left(-\frac{1}{2}\sqrt{\frac{L_{\text{B}}}{C_{\text{B}}}}\right), \qquad J_{\text{Potts}} = \frac{1}{2L_{\text{Potts}}}\sqrt{\frac{L_{\text{B}}}{C_{\text{B}}}}. \tag{31}$$

C. Coupled optomechanical $\mathbb{Z}_3$ Rabi models

We can repeat the same procedure for the optomechanical system. However, it is a bit more peculiar, because of the circular waveguide in the optomechanical Rabi model. To build the optomechanical $\mathbb{Z}_3$ Potts model we arrange the optomechanical $\mathbb{Z}_3$ Rabi model concentrically (see Fig. 4). On the one hand, the radius of the waveguide does not affect the parameters of the model, on the other hand, placing the ions of the neighbor Rabi models close to each other creates phonon-phonon interaction through the ion Coulomb interaction [61, 62]. The phonon-phonon interaction between the neighboring Rabi models leads to the Hamiltonian (24) and consequently to the $\mathbb{Z}_3$ Potts model as described before.

D. Chiral Potts model and parafermions

In this subsection, we want to briefly overview the chiral Potts model. It is a generalization of the ordinary

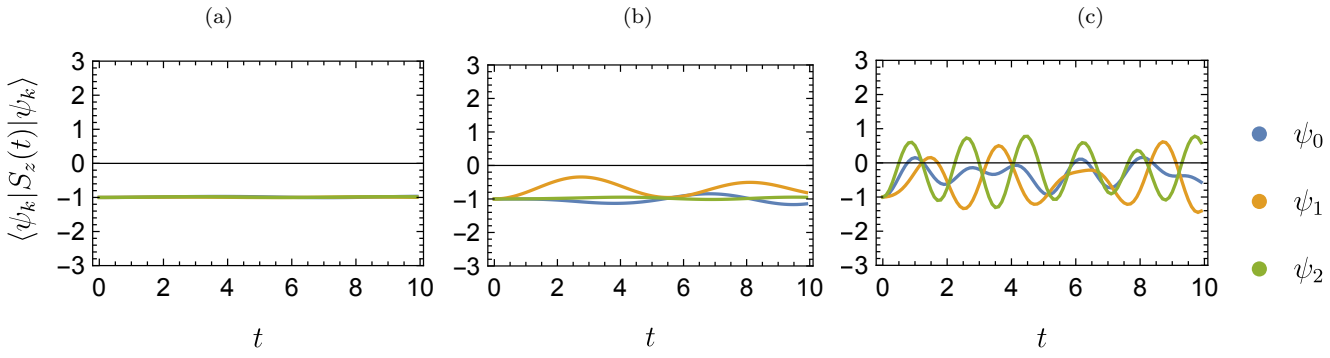

FIG. 5. Time dependence of the total spin excitation operator. To illustrate robustness of the Rabi model implementation with the respect of disorder (37) we plotted $\langle S_z(t)\rangle$. The standard variance of the disorder Δ_j equals for plot a) 0.1; b) 0.3; c) 1.

Potts model that has a chiral nearest-neighbour interaction:

$$\begin{aligned} H_{\text{chPotts}} =& f' \sum_{n=1}^{L} (e^{i\phi'} Z_n + e^{-i\phi'} Z_n^\dagger) \\ &+ J' \sum (e^{i\theta'} X_n X_{n+1}^\dagger + e^{-i\theta'} X_n^\dagger X_{n+1}). \end{aligned} \tag{32}$$

It is simply the Potts model (23) with a complex parameter J'.

The chiral Potts model exhibits richer physics compared to the ordinary one. In particular, it can host parafermion physics. We discuss it more below, but first, we need to discuss how to obtain this chiral interaction, because it is quite challenging.

As mentioned earlier, the interaction parameter J' originates from the neighbor $\mathbb{Z}_3$ Rabi models boson interaction. Hence, if we want to obtain the chiral Potts model, we have to obtain a chiral boson-hopping term. The full technical discussion of this topic is outside of this paper's scope. However, we want to mention that recently a way to obtain the chiral boson hopping was proposed in [63], and we assume that it could be adapted to our system.

For the Potts system a certain generalization of the Jordan-Wigner transformation exists. It is called the Fradkin-Kadanoff (FK) transformation [30], and it allows us to rewrite X_j, Z_j in terms of parafermions:

$$\Gamma_j = \prod_{k<j} Z_k X_j, \quad \Delta_j = \prod_{k\leq j} Z_k X_j. \tag{33}$$

Here Γ_j, Δ_j are parafermion operators with a parafermion commutation relation: $\Gamma_j\Gamma_k = \omega^{\text{sign}(j-k)}\Gamma_k\Gamma_j$, $\Delta_j\Delta_k = \omega^{\text{sign}(j-k)}\Delta_k\Delta_j$, and finally $\Gamma_j\Delta_k = \omega^{\text{sign}(j-k)}\Delta_k\Gamma_j$.

Using the FK transformation, it is easy to show that the Potts model is equivalent to a parafermion chain. The only problem is that FK transformation is not local. In terms of parafermion operators, the chiral Potts model Hamiltonian (32) looks like

$$\begin{aligned} H_{\text{chPotts}} =& f' \sum \left(e^{i\phi'}\Gamma_j\Delta_j^\dagger + e^{-i\phi'}\Delta_j\Gamma_j^\dagger\right) \\ &+ J' \sum \left(e^{i\theta'}\Delta_j\Gamma_{j+1}^\dagger + e^{-i\theta'}\Gamma_{j+1}\Delta_j^\dagger\right) \end{aligned} \tag{34}$$

On the other hand, it is known that parafermion chain has a phase with a parafermion edge mode [6]:

$$\Gamma_{\text{edge}} = \Gamma_1 + \frac{f'}{J'\sin(3\theta')}\mathcal{O} + \dots \tag{35}$$

Unfortunately, after the parafermion edge mode is not localized on the edged after FK transformation. As a result, we do not have an actual topological phase in the chiral Potts model. But we believe that it still holds an importance because it allows us to simulate a parafermion chain.

IV. DISORDER IN THE SUPERCONDUCTING IMPLEMENTATION

A. Disorder breaking the total qubit excitation number conservation

First, while discussing the effect of the disorder on the qubit-boson ring (1), we need to consider a term that breaks the conservation of the total excitation number of qubits $\hat{S}^z$. This conservation law is broken by the Zeeman terms being not perfectly aligned with $\hat{z}$ direction:

$$\hat{H}_{QB,\text{dis}} = \hat{H}_{QB} + \sum_{j=1}^{3} \Delta_j \sigma_j^x. \tag{36}$$

As explained in App. B, Δ_j being equal to zero for qubit-boson ring based on superconducting circuits relies on the fine-tuning of the SQUID magnetic field. Therefore, in a realistic setting we unavoidably are going to have non-zero $\Delta_j = I_{Q,1}\sin(\Delta\Phi_j)$.

As a result, we have $[\hat{H}_{QB,\text{dis}}, \hat{S}^z] \neq 0$. Unfortunately, it breaks the derivation of the Rabi model. However,

assuming that the disorder is considerably smaller then other parameters in the Hamiltonian, we can still hope that the dynamics is approximately governed by the Rabi model. Because an analytic estimate is cumbersome, we performed numerical simulations of the qubit–boson ring. The results could be seen on Fig. 5. The simulation shows that for the small disorder the qubit-boson ring stays around the single excitation subspace $\mathcal{H}_1$ because $\langle \hat{S}^z \rangle(t) \approx 1$. We speculate that it happens because the spins precess around $\langle \hat{S}^z \rangle = 1$.

B. Disorder breaking $\mathbb{Z}_3$ symmetry

Now, assuming that the total number of qubit excitations is conserved, we would like to investigate how the coordinate dependence of the parameter in the qubit-boson ring influences the resulting Rabi model. The spatial non-homogeneity obviously breaks the $\mathbb{Z}_3$ symmetry. However, we want to find the explicit symmetry-breaking term.

$$\begin{aligned}\hat{H}'_{QB} = &\sum_j \epsilon_j \sigma_j^z + \sum_j \Omega_j \hat{a}_j^\dagger \hat{a}_j \\ &+ \sum_j g_{j,j+1} \left[\sigma_j^+ \sigma_{j+1}^- e^{i(\hat{x}_j - \hat{x}_{j+1})} + \text{h.c}\right]\end{aligned} \tag{37}$$

where we have

$$\begin{aligned}&\epsilon_j = \frac{\delta_j}{2C_{Q,j}},\ \Omega_{QB,j} = \left(L_{\mathrm{B},j} C_{\mathrm{B},j}\right)^{-1/2}, \\ &g_{j,j+1} = \frac{I_{\mathrm{Rabi},j}}{2}.\end{aligned} \tag{38}$$

For brevity, we decompose the coupling parameters into a homogeneous part and a disorder: $\epsilon_j = \epsilon + \Delta\epsilon_j$, $\Omega_j = \Omega + \Delta\Omega_j$, $g_{j,j+1} = g + \Delta g_{j,j+1}$, where we assume that the disorder averaged over the coordinate is zero: $\sum_j \Delta\epsilon_j = \sum_j \Delta\Omega_j = \sum_j \Delta g_{j,j+1} = 0$. We can always achieve this by adjusting the homogeneous coupling.

Then the single-excitation sector is going to be described by

$$\begin{aligned}&\hat{H}'_{2\ \mathrm{Rabi}} = \hat{H}_{2\ \mathrm{Rabi}} + \epsilon(2)X \\ &+ \epsilon(1)X^\dagger + (X + X^\dagger)\sum_{k=1}^{2} \Delta g(k) Z^k \\ &+ \Omega(1)\sum_{k=0}^{2} \hat{a}^\dagger(k+1)\hat{a}(k) + \Omega(2)\sum_{k=0}^{2} \hat{a}^\dagger(k)\hat{a}(k+1) \\ &+ \sum_{l=1}^{2} \frac{\Omega^{3/2}(l)}{2^{3/2}} \sum_{k=0}^{2} (\hat{a}(k+l) + \hat{a}^\dagger(-k-l)) Z^k.\end{aligned} \tag{39}$$

Due to the disorder the first boson mode does not decouple anymore. However, the structure of threefold cat state should be still conserved for small disorder.

V. CONCLUSION

We have explored $\mathbb{Z}_3$-symmetric models, with a particular focus on the $\mathbb{Z}_3$ Rabi model and its variations. By employing a canonical transformation, we successfully derived the spectrum of these models, revealing that the three lowest eigenstates correspond to distinct threefold cat states, a feature interesting from several perspectives. We derived an analytical expression for the Wigner quasi-probability function of the threefold cat state and used it to better understand the structure of the cat states.

We also introduced a hierarchy of $\mathbb{Z}_3$-symmetric systems. In the qubit-boson ring, the $\mathbb{Z}_3$ symmetry appears as a discrete rotational symmetry, whereas in the Rabi model, a specific sector of the qubit-boson ring, the symmetry acts as an internal one. This internal symmetry also exists in the $\mathbb{Z}_3$ Potts model, which we constructed by coupling multiple $\mathbb{Z}_3$ Rabi models.

Our main goal was to suggest a way towards an experimental realization of the $\mathbb{Z}_3$ Rabi and Potts models. We believe that the proposed superconducting circuit should be feasible to implement. However, this approach does not have to be restricted only to the superconducting circuit platform. For example, we believe that a similar strategy work for the spin-qubit systems. Though, this remains a topic for a future research.

More broadly, our work highlights the intriguing potential of $\mathbb{Z}_n$-symmetric systems within condensed matter physics. These systems present a fertile ground for discovering novel quantum phenomena, many of which are yet to be fully understood or described. We believe that the further investigation into these models reveals new insights and advance our understanding of symmetry in quantum systems.

ACKNOWLEDGMENTS

We thank Daria Kalacheva, Henry Legg, Katharina Laubscher, and Ilia Luchnikov for fruitful discussions and useful comments. This work was supported as a part of NCCR SPIN, a National Centre of Competence in Research, funded by the Swiss National Science Foundation (grant number 225153). This work has received funding from the Swiss State Secretariat for Education, Research and Innovation (SERI) under contract number M822.00078.

Appendix A: Generalisation to an arbitrary interaction matrix

For completeness we summarise how the above derivation extends to a QB ring with an arbitrary $\mathbb{Z}_3$–symmetric interaction matrix A. The starting Hamil-

tonian is

$$\begin{aligned}\hat{H}_{\rm gen} &= \epsilon\sum_{j=1}^{3}\sigma_j^z + \Omega\sum_{j=1}^{3}\hat{a}_j^\dagger\hat{a}_j + \hat{V}_{\rm gen},\\ \hat{V}_{\rm gen} &= g\sum_{j,k}A_{jk}\sigma_j^+\sigma_k^- e^{i(\hat{x}_j-\hat{x}_k)},\end{aligned} \tag{A1}$$

with $A^\dagger = A$. The same sequence of steps—momentum translation S, Fourier transform, and restriction to $\mathcal{H}_{\rm QB,1}$—again leads to the two–mode Hamiltonian[31] (7), now with gA replacing $g(Z+Z^\dagger)$. Hence any interaction matrix compatible with $\mathbb{Z}_3$ symmetry can be mapped onto the canonical Rabi model. The parameter correspondence reads

$$\Omega_R = \Omega, \qquad \lambda = \sqrt{\frac{\Omega}{6m}}. \tag{A2}$$

In the superconducting implementation one has $A = X+X^\dagger$, thereby recovering the special case treated above. The optomechanical realisation gives rise to a different Hermitian A but follows exactly the same logic.

Appendix B: Charge qubit for the $\mathbb{Z}_3$ Rabi model

The Cooper Pair Box (CPB) qubit is the most well-known type of charge qubit. However, it is not suitable for our purposes because its eigenstates are not charge states but their symmetric/antisymmetric combinations. Its Hamiltonian is proportional to σ^x. But in this case, the qubit chain Hamiltonian does not commute with total number of qubit excitations operator S^z.

Hence, we need another type of a charge qubit. Considering that the σ^x term in the Hamiltonian arises from the JJ term the natural idea is to get rid of the JJ and consider a purely capacitor qubit. Although theoretically suitable for our purposes, without the JJ the charge qubit is very sensitive to noise. Therefore, it is not a realistic approach.

Consequently, we want two things simultaneously: Hamiltonian proportional to σ^z in charge basis and JJ to fight noise. The solution turns out to be a higher harmonic Josephson junction. Usually it is neglected, but the JJ Hamiltonian always include higher harmonics as well

$$\hat{H}_{JJ} = E_{J,1}\cos\hat{\phi} + E_{J,2}\cos 2\hat{\phi} + \dots, \tag{B1}$$

where ϕ is the superconducting phase.

In practice, the higher harmonics are usually considerably weaker $E_{J,2} \ll E_{J,1}$. But if we were to eliminate the first harmonic completely, then we would be left with the second harmonic. The second harmonic, on the one hand, can help to supress the noise and, on the other hand, does not appear in the qubit Hamiltonian:

$$\cos 2\hat{\phi}\Big|_{\mathcal{V}} = \frac{1}{2}\left(e^{2i\hat{\phi}} + e^{-2i\hat{\phi}}\right)\Big|_{\mathcal{V}} = \frac{1}{2}\left((\sigma^+)^2 + (\sigma^-)^2\right) = 0 \tag{B2}$$

To eliminate the first harmonic, we can use a Superconducting Quantum Interference Device (SQUID) [64]. If the magnetic flux through the SQUID is tuned to $\Phi = \pi$, then the SQUID Hamiltonian looks like:

$$\begin{aligned}\hat{H}_{squid} =& I_{Q,1}\cos\left(\hat{\phi}\right) + I_{Q,2}\cos\left(2\hat{\phi}\right) + I_{Q,1}\cos\left(\hat{\phi}+\pi\right)\\ &+ I_{Q,2}\cos\left(2\hat{\phi}+2\pi\right) = 2I_{Q,2}\cos\left(2\hat{\phi}\right).\end{aligned} \tag{B3}$$

As a result, only the second harmonic is left.

Consequently, we can construct a qubit based on the second-harmonic JJ (see Fig. **??**). It is described by the Hamiltonian:

$$\hat{H} = \frac{1}{2C_Q}(\hat{n}-n_0)^2 + 2I_{Q,2}\cos\left(2\hat{\phi}\right) \tag{B4}$$

If we tune n_0 a bit off 1/2: $n_0 = 0.5-\delta$, then the qubit Hamiltonian looks like:

$$\hat{H}_{\rm qubit} = \frac{\delta}{2C_Q}\sigma_z. \tag{B5}$$

Hence, we obtained the qubit Hamiltonian we wanted. Here we consider $\frac{1}{2C} \gg 2E_{J,2}$ as usual for charge qubits.

To conclude, the charge qubit we have in mind consists of a capacitor and the second-harmonic JJ. One can think of it as a certain generalization of a Cooper Pair Box qubit. In this appendix, we only briefly described its blueprint to give additional substance to the proposal in Sec. II B.

[1] F. Y. Wu, The Potts model, Rev. Mod. Phys. **54**, 235 (1982).

[2] C. M. Fortuin and P. W. Kasteleyn, On the random-cluster model: I. Introduction and relation to other models, Physica **57**, 536 (1972).

[3] H. N. V. Temperley, E. H. Lieb, and S. F. Edwards, Relations between the 'percolation' and 'colouring' problem and other graph-theoretical problems associated with regular planar lattices: Some exact results for the 'percolation' problem, Proc. R. Soc. Lond. Math. Phys. Sci. **322**, 251 (1971).

[4] R. J. Baxter, J. H. H. Perk, and H. Au-Yang, New solutions of the star-triangle relations for the chiral potts model, Physics Letters A **128**, 138 (1988).

[5] P. Fendley, Free parafermions, J. Phys. Math. Theor. **47**, 075001 (2013).

[6] P. Fendley, Parafermionic edge zero modes in Zn-invariant spin chains, J. Stat. Mech. **2012**, P11020

(2012).
[7] R. L. R. C. Teixeira and L. G. G. V. Dias da Silva, Edge ${\mathbb{Z}}_{3}$ parafermions in fermionic lattices, Phys. Rev. B **105**, 195121 (2022).
[8] J. Alicea and P. Fendley, Topological Phases with Parafermions: Theory and Blueprints, Annu. Rev. Condens. Matter Phys. **7**, 119 (2016).
[9] E. Cobanera and G. Ortiz, Fock parafermions and self-dual representations of the braid group, Phys. Rev. A **89**, 012328 (2014).
[10] Y. Wang, Z. Hu, B. C. Sanders, and S. Kais, Qudits and High-Dimensional Quantum Computing, Front. Phys. **8**, 589504 (2020).
[11] E. O. Kiktenko, A. K. Fedorov, A. A. Strakhov, and V. I. Man'ko, Single qudit realization of the Deutsch algorithm using superconducting many-level quantum circuits, Physics Letters A **379**, 1409 (2015).
[12] E. O. Kiktenko, A. S. Nikolaeva, P. Xu, G. V. Shlyapnikov, and A. K. Fedorov, Scalable quantum computing with qudits on a graph, Phys. Rev. A **101**, 022304 (2020).
[13] T. J. Proctor, Quantum information with general quantum variables: A formalism encompassing qubits, qudits, and quantum continuous variables (2019), arXiv:1903.08545 [quant-ph].
[14] J. M. Farinholt, An Ideal Characterization of the Clifford Operators, J. Phys. A: Math. Theor. **47**, 305303 (2014).
[15] J.-L. Brylinski and R. Brylinski, Universal quantum gates (2001), arXiv:quant-ph/0108062.
[16] J. Braumüller, M. Marthaler, A. Schneider, A. Stehli, H. Rotzinger, M. Weides, and A. V. Ustinov, Analog quantum simulation of the Rabi model in the ultra-strong coupling regime, Nat Commun **8**, 779 (2017).
[17] D. Braak, Integrability of the Rabi Model, Phys. Rev. Lett. **107**, 100401 (2011).
[18] M.-J. Hwang, R. Puebla, and M. B. Plenio, Quantum Phase Transition and Universal Dynamics in the Rabi Model, Phys. Rev. Lett. **115**, 180404 (2015).
[19] Y.-H. Chen, W. Qin, X. Wang, A. Miranowicz, and F. Nori, Shortcuts to Adiabaticity for the Quantum Rabi Model: Efficient Generation of Giant Entangled Cat States via Parametric Amplification, Phys. Rev. Lett. **126**, 023602 (2021).
[20] V. V. Albert, Quantum Rabi Model for N -State Atoms, Phys. Rev. Lett. **108**, 180401 (2012).
[21] Y.-Z. Zhang, Z_N symmetric chiral Rabi model: A new N-level system, Annals of Physics **347**, 122 (2014).
[22] D. Sedov, V. Kozin, and I. Iorsh, Chiral Waveguide Optomechanics: First Order Quantum Phase Transitions with ${\mathbb{Z}}_{3}$ Symmetry Breaking, Phys. Rev. Lett. **125**, 263606 (2020).
[23] B. Vlastakis, G. Kirchmair, Z. Leghtas, S. E. Nigg, L. Frunzio, S. M. Girvin, M. Mirrahimi, M. H. Devoret, and R. J. Schoelkopf, Deterministically Encoding Quantum Information Using 100-Photon Schrödinger Cat States, Science **342**, 607 (2013).
[24] J. M. C. Malbouisson and B. Baseia, Higher-generation Schrödinger cat states in cavity QED, J. Mod. Opt. **46**, 2015 (1999).
[25] M. Bergmann and P. van Loock, Quantum error correction against photon loss using multicomponent cat states, Phys. Rev. A **94**, 042332 (2016).
[26] A. Grimm, N. E. Frattini, S. Puri, S. O. Mundhada, S. Touzard, M. Mirrahimi, S. M. Girvin, S. Shankar, and M. H. Devoret, Stabilization and operation of a Kerr-cat qubit, Nature **584**, 205 (2020).
[27] J. Guillaud and M. Mirrahimi, Repetition Cat Qubits for Fault-Tolerant Quantum Computation, Phys. Rev. X **9**, 041053 (2019).
[28] M.-J. Hwang and M.-S. Choi, Large-scale maximal entanglement and Majorana bound states in coupled circuit quantum electrodynamic systems, Phys. Rev. B **87**, 125404 (2013).
[29] M. M. Wauters, L. Maffi, and M. Burrello, Engineering a Josephson junction chain for the simulation of the clock model (2024), arXiv:2408.14549 [cond-mat, physics:quant-ph].
[30] E. Fradkin and L. P. Kadanoff, Disorder variables and para-fermions in two-dimensional statistical mechanics, Nuclear Physics B **170**, 1 (1980).
[31] We use brackets to denote the Fourier-transformed operators' dependence on the wavevector. On the other hand, for real space operators we use subscripts for their coordinate dependence as usual.
[32] B. Yurke and J. S. Denker, Quantum network theory, Phys. Rev. A **29**, 1419 (1984).
[33] M. Devoret, *Quantum Fluctuations in Electrical Circuits* (Edition de Physique, France, 1997).
[34] G. Wendin and V. S. Shumeiko, Superconducting Quantum Circuits, Qubits and Computing (2005), arXiv:cond-mat/0508729.
[35] S. Bosco, P. Scarlino, J. Klinovaja, and D. Loss, Fully Tunable Longitudinal Spin-Photon Interactions in Si and Ge Quantum Dots, Phys. Rev. Lett. **129**, 066801 (2022).
[36] S. Felicetti, G. Romero, E. Solano, and C. Sabín, Quantum Rabi model in a superfluid Bose-Einstein condensate, Phys. Rev. A **96**, 033839 (2017).
[37] I. C. Skogvoll, J. Lidal, J. Danon, and A. Kamra, Tunable Anisotropic Quantum Rabi Model via a Magnon–Spin-Qubit Ensemble, Phys. Rev. Applied **16**, 064008 (2021).
[38] T. Niemczyk, F. Deppe, H. Huebl, E. P. Menzel, F. Hocke, M. J. Schwarz, J. J. Garcia-Ripoll, D. Zueco, T. Hümmer, E. Solano, A. Marx, and R. Gross, Circuit quantum electrodynamics in the ultrastrong-coupling regime, Nature Phys **6**, 772 (2010).
[39] P. Forn-Díaz, J. J. García-Ripoll, B. Peropadre, J.-L. Orgiazzi, M. A. Yurtalan, R. Belyansky, C. M. Wilson, and A. Lupascu, Ultrastrong coupling of a single artificial atom to an electromagnetic continuum in the nonperturbative regime, Nature Phys **13**, 39 (2017).
[40] F. Yoshihara, T. Fuse, S. Ashhab, K. Kakuyanagi, S. Saito, and K. Semba, Superconducting qubit–oscillator circuit beyond the ultrastrong-coupling regime, Nature Phys **13**, 44 (2017).
[41] E. Vlasiuk, V. K. Kozin, J. Klinovaja, D. Loss, I. V. Iorsh, and I. V. Tokatly, Cavity-induced charge transfer in periodic systems: Length-gauge formalism, Phys. Rev. B **108**, 085410 (2023).
[42] V. K. Kozin, D. Miserev, D. Loss, and J. Klinovaja, Quantum phase transitions and cat states in cavity-coupled quantum dots, Phys. Rev. Res. **6**, 033188 (2024).
[43] Z. Chen, Y. Wang, T. Li, L. Tian, Y. Qiu, K. Inomata, F. Yoshihara, S. Han, F. Nori, J. S. Tsai, and J. Q. You, Single-photon-driven high-order sideband transitions in an ultrastrongly coupled circuit-quantum-electrodynamics system, Phys. Rev. A **96**, 012325 (2017).
[44] L. S. Ricco, V. K. Kozin, A. C. Seridonio, and I. A. Shelykh, Reshaping the jaynes-cummings ladder with majorana bound states, Phys. Rev. A **106**, 023702 (2022).

[45] A. Hutter, J. R. Wootton, and D. Loss, Parafermions in a Kagome Lattice of Qubits for Topological Quantum Computation, Phys. Rev. X **5**, 041040 (2015).

[46] V. Bouchiat, D. Vion, P. Joyez, D. Esteve, and M. H. Devoret, Quantum coherence with a single Cooper pair, Phys. Scr. **1998**, 165 (1998).

[47] Y. Nakamura, Y. A. Pashkin, and J. S. Tsai, Coherent control of macroscopic quantum states in a single-Cooper-pair box, Nature **398**, 786 (1999).

[48] K. W. Lehnert, K. Bladh, L. F. Spietz, D. Gunnarsson, D. I. Schuster, P. Delsing, and R. J. Schoelkopf, Measurement of the Excited-State Lifetime of a Microelectronic Circuit, Phys. Rev. Lett. **90**, 027002 (2003).

[49] Y. Makhlin, G. Schön, and A. Shnirman, Quantum-state engineering with Josephson-junction devices, Rev. Mod. Phys. **73**, 357 (2001).

[50] J. Siewert, R. Fazio, G. M. Palma, and E. Sciacca, Aspects of Qubit Dynamics in the Presence of Leakage, Journal of Low Temperature Physics **118**, 795 (2000).

[51] S. E. Rasmussen, K. S. Christensen, and N. T. Zinner, Controllable two-qubit swapping gate using superconducting circuits, Phys. Rev. B **99**, 134508 (2019).

[52] S. E. Shafranjuk, Two-qubit gate based on a multiterminal double-barrier Josephson junction, Phys. Rev. B **74**, 024521 (2006).

[53] M. Allman, J. Whittaker, M. Castellanos-Beltran, K. Cicak, F. da Silva, M. DeFeo, F. Lecocq, A. Sirois, J. Teufel, J. Aumentado, and R. Simmonds, Tunable Resonant and Nonresonant Interactions between a Phase Qubit and LC Resonator, Phys. Rev. Lett. **112**, 123601 (2014).

[54] Y. Hu, Y.-F. Xiao, Z.-W. Zhou, and G.-C. Guo, Controllable coupling of superconducting transmission-line resonators, Phys. Rev. A **75**, 012314 (2007).

[55] S. Bravyi, D. P. DiVincenzo, and D. Loss, Schrieffer–Wolff transformation for quantum many-body systems, Annals of Physics **326**, 2793 (2011).

[56] R. J. Baxter, Critical Antiferromagnetic Square-Lattice Potts Model, Proc. R. Soc. Lond. Ser. Math. Phys. Sci. **383**, 43 (1982).

[57] D. Aharonov, I. Arad, E. Eban, and Z. Landau, Polynomial Quantum Algorithms for Additive approximations of the Potts model and other Points of the Tutte Plane (2007), arXiv:quant-ph/0702008.

[58] S. Okada, M. Ohzeki, and K. Tanaka, Efficient quantum and simulated annealing of Potts models using a half-hot constraint (2019).

[59] V. K. Kozin, E. Thingstad, D. Loss, and J. Klinovaja, Cavity-enhanced superconductivity via band engineering, Phys. Rev. B **111**, 035410 (2025).

[60] V. K. Kozin, D. Miserev, D. Loss, and J. Klinovaja, Schottky anomaly in a cavity-coupled double quantum well (2025), arXiv:2504.08630 [cond-mat.mes-hall].

[61] C. Schneider, D. Porras, and T. Schaetz, Experimental quantum simulations of many-body physics with trapped ions, Rep. Prog. Phys. **75**, 024401 (2012).

[62] L. Timm, *Dynamics of Ion Coulomb Crystals*, DoctoralThesis, Hannover : Institutionelles Repositorium der Leibniz Universität Hannover (2023).

[63] A. Bermudez, T. Schaetz, and D. Porras, Synthetic Gauge Fields for Vibrational Excitations of Trapped ions, Phys. Rev. Lett. **107**, 150501 (2011).

[64] M. Valentini, O. Sagi, L. Baghumyan, T. de Gijsel, J. Jung, S. Calcaterra, A. Ballabio, J. Aguilera Servin, K. Aggarwal, M. Janik, T. Adletzberger, R. Seoane Souto, M. Leijnse, J. Danon, C. Schrade, E. Bakkers, D. Chrastina, G. Isella, and G. Katsaros, Parity-conserving Cooper-pair transport and ideal superconducting diode in planar germanium, Nat Commun **15**, 169 (2024).